THE JOURNAL OF PHYSICAL CHEMISTRY Letters

Letter

pubs.acs.org/JPCL

The Role of Hydrogen Bonds in the Stabilization of Silver-Mediated Cytosine Tetramers

Leonardo Andrés Espinosa Leal,[†] Alexander Karpenko,[†] Steven Swasey,[‡] Elisabeth G. Gwinn,[§] Victor Rojas-Cervellera,[∥] Carme Rovira,[∥] and Olga Lopez-Acevedo*[,†]

[†]COMP Centre of Excellence, Department of Applied Physics, Aalto University, P.O. Box 11100, 00076 Aalto, Finland

[‡]Department of Chemistry and Biochemistry, University of California, Santa Barbara, California 93106-9510, United States

[§]Department of Physics, University of California, Santa Barbara, California 93106-9510, United States

[∥]Departament de Química Orgànica & Institut de Química Teòrica I Computacional (IQTCUB), Universitat de Barcelona, Martí I Franquès 1, 08208 Barcelona, Spain

Supporting Information

ABSTRACT: DNA oligomers can form silver-mediated duplexes, stable in gas phase and solution, with potential for novel biomedical and technological applications. The nucleobase-metal bond primarily drives duplex formation, but hydrogen (H−) bonds may also be important for structure selection and stability. To elucidate the role of H-bonding, we conducted theoretical and experimental studies of a duplex formed by silver-mediated cytosine homopobase DNA strands, two bases long. This silver-mediated cytosine tetramer is small enough to permit accurate, realistic modeling by DFT-based quantum mechanics/molecular mechanics methods. In gas phase, our calculations found two energetically favorable configurations distinguished by H-bonding, one with a novel interplane H-bond, and the other with planar H-bonding of silver-bridged bases. Adding solvent favored silver-mediated tetramers with interplane H-bonding. Overall agreement of electronic circular dichroism spectra for the final calculated structure and experiment validates these findings. Our results can guide use of these stabilization mechanisms for devising novel metal-mediated DNA structures.

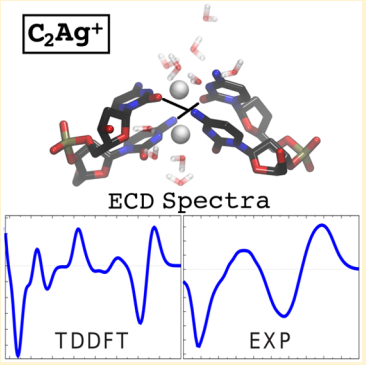

Recent experimental advances in the field of metal−DNA interactions have attracted attention due to their possible biomedical and technological applications, such as nano-conductors, magnetic storage,[1] nanophotonics,[2,3] toxic metals detection,[4] and DNA sequencing[5] among others.[6−8] Among these advances, some occurred using modified DNA with synthetic nucleobases.[9−11] However, proof has emerged in the past few years that Ag^+ can form duplexes of natural DNA strands via cytosine-Ag^+-cytosine, guanine-Ag^+-guanine, and adenine-Ag^+-thymine pairings.[12−14] In the case of cytosine mismatches embedded in otherwise complementary DNA strands, experiments found that the constraints imposed by Watson−Crick pairing of the surrounding duplex preserved the antiparallel strand orientation upon formation of the cytosine-Ag^+-cytosine pair.[12] In the conformationally unconstrained conditions discussed in this Letter, silver-mediated duplexes of cytosine dinucleotides are evidenced to be most stable in parallel strand orientation corresponding to a *trans* configuration of the bases (Figure 1), as is also supported experimentally.[13−15] In solution, DNA double-helical strands are stabilized mainly via H-bonds and π-stacking interactions. In silver-mediated DNA duplexes, several more interactions come into play. Silver cations interact strongly with nitrogen and oxygen atoms on the nucleobases, following simple electrostatic rules and with calculated strengths of 100 kcal/mol for Ag^+-bridged bases in vacuum, roughly 4 times the binding energy of a canonical H-bonded C-G base pair and 10 times that for a canonical A−T pair calculated at the same level of theory.[14,16] Experiments on aqueous solutions found silver-mediated base pairings with high thermal stability, up to 90 °C according to circular dichroism spectra for cytosine homopolymer strands only 6 bases in length.[14] Although binding

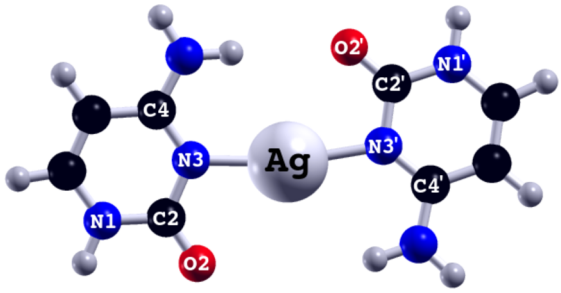

Figure 1. Ground state of cytosine-Ag^+-cytosine complex with the two cytosines in a *trans* configuration with the silver cation bonded to the central nitrogen atoms and with one planar H-bond.

Received: August 26, 2015
Accepted: September 24, 2015
Published: September 24, 2015

DOI: 10.1021/acs.jpclett.5b01864
J. Phys. Chem. Lett. 2015, 6, 4061−4066

energies of H-bonds are much weaker than the metal−base interactions, H-bonding will remain an important interaction for tuning overall structure, particularly in solution, where entropic contributions to the free energy are significant. While computational studies of simple nucleobase−metal−nucleobase complexes in vacuum show that H-bonds help stabilize particular isomers,[14,17] one can only expect to understand the role of H-bonding in solution from a realistic model including backbone and a solvent that examines both π-stacking and metallophilic interaction effects on the structure. In particular, some have suggested that metallophilic interactions play an added role not only in the stability, but also in the luminescence properties of silver(I) compounds.[18]

Structural arrangements in these new metal−DNA hybrids are particularly difficult to obtain experimentally via crystallization.[19] Therefore, theoretical calculations using quantum chemistry methods appear as the most promising tool to propose geometries and interpret the experimental data. Experimentally, electronic circular dichroism (ECD) spectroscopy is the preferred tool used in characterizing DNA's secondary (and higher) structure, because this technique is highly sensitive to small geometric changes. Hence, we extended this method to study the ECD signatures of silver-mediated cytosine duplexes, with four cytosine bases total, which we call Ag^+-bridged or silver-mediated cytosine tetramers below. Calculations of the excited states of DNA, in particular optical absorption spectroscopy of nanostructures, have been carried out successfully in the past using different computational methodologies.[20−22] However, modeling ECD in DNA using *ab initio* methods is a difficult task (*vide supra*). Simulating the ECD for a silver-mediated tetramer of cytosine then represents a challenge that requires appropriate density functional theory (DFT) techniques. For instance, interactions present in DNA such as H-bonding and π-stacking are inaccurately estimated with standard DFT functionals; they need the inclusion of van der Waals (vdW)-DFT corrections.[23] Metallophilic interactions and cation−π interactions are potentially present, and therefore we must test the vdW-DFT functionals. Moreover, once we include the solvent, the system's size is prohibitive for a full quantum calculation, and thus requires multiscale strategies such as hybrid quantum and molecular mechanics (QM/MM). Finally, charge-transfer excitations are poorly described with standard DFT functionals, so hybrid or long-range corrected DFT functionals are required. Here, we report the first complete analysis of the structure of an Ag^+-bridged cytosine tetramer through a combined theoretical and experimental study. The study's purpose is to obtain the underlying physicochemical stabilization mechanisms with the use of accurate and realistic computational methods validated by experiment.

The vacuum ground-state of the Ag^+-bridged cytosine dimer (i.e., the cytosine-Ag^+-cytosine complex) has the two cytosines in a trans configuration with the silver cation bonded to the central nitrogen atoms and with one interbase H-bond favoring the overall planarity[15,17] (see Figure 1). Henceforth, we denote this interbase bond in overall planar symmetry as a *planar H-bond*. This type of structure was reported recently[24] as a possible model for the Ag^+-bridged cytosine tetramer from a quantum dynamics simulation at room temperature with implicit water. The stable planar H-bonded tetramer has one planar H-bond out of the four possible (see bottom of Figure 2A) and a Ag−Ag distance of about 3.9 Å. We optimized this planar H-bonded structure with vdW-corrected PBE functional

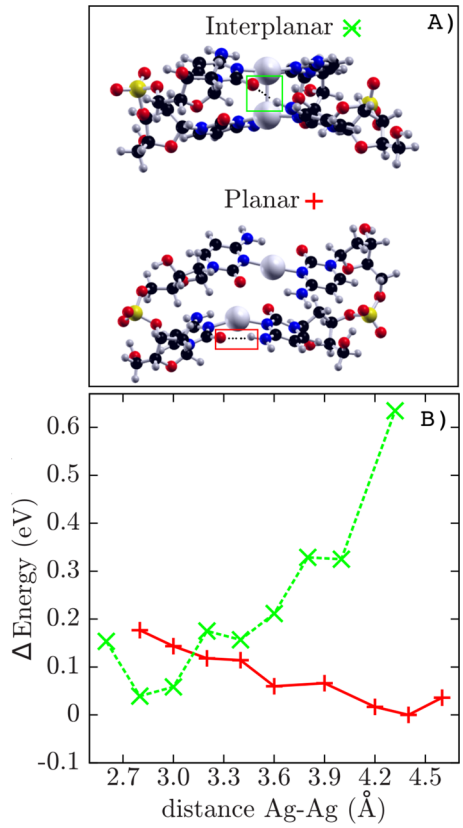

Figure 2. (A) Two minimal Ag^+-bridged cytosine tetramers in gas-phase with interplanar H-bond and planar H-bond reoptimized from the work of Fortino et al.[24] (B) Total energy obtained from different minimizations keeping constant the Ag−Ag distance. We use DFT at the PBE+TS09 level by using the Minima Hopping algorithm. The green line corresponds to structures similar to the upper, interplanar form and the red line to structures similar to the lower, planar form.

(PBE+TS09[25,26]) in vacuum and obtained similar results, but with a longer Ag−Ag distance (4.2 Å), where no metallophilic interaction is expected.[27]

To explore the possible role of metallophilicity, we began with a structure with planar H-bonds but shorter Ag−Ag distance (2.8 Å) as the input of a Minima Hopping algorithm (Supporting Information (SI)).[28] Our optimization found a new type of H-bond that links the bases of different planes of the duplex (see top of Figure 2A and SI for the optimization's details). We denote this bond as an *interplanar hydrogen bond*. We stretched both structures by changing the distance between silver atoms by 0.2 Å per step, and we applied the Minima Hopping optimization, while keeping the silver atoms' positions constant. Figure 2B shows the results of the total energy versus the Ag−Ag distance. The procedure of changing the Ag−Ag distance by small steps preserves the overall structure, type, and number of H-bonds; meanwhile, the dihedral angles formed between the cytosines, and the silver ions can change when the geometry approaches its energetic minima (see SI). At larger distances, the tetramer with a planar H-bond is lower in energy and has a minimum at around 4.4 Å, while at shorter Ag−Ag distances, the interplanar H-bond structure is preferred and has a minimum at around 2.8 Å. Thus, in the gas phase, there are two energetically favorable, stable structures differentiated by the expected Ag−Ag distance and the H-bond configuration. The interplanar H-bond stabilizes the tetramer at short Ag−Ag

DOI: 10.1021/acs.jpclett.5b01864
J. Phys. Chem. Lett. 2015, 6, 4061−4066

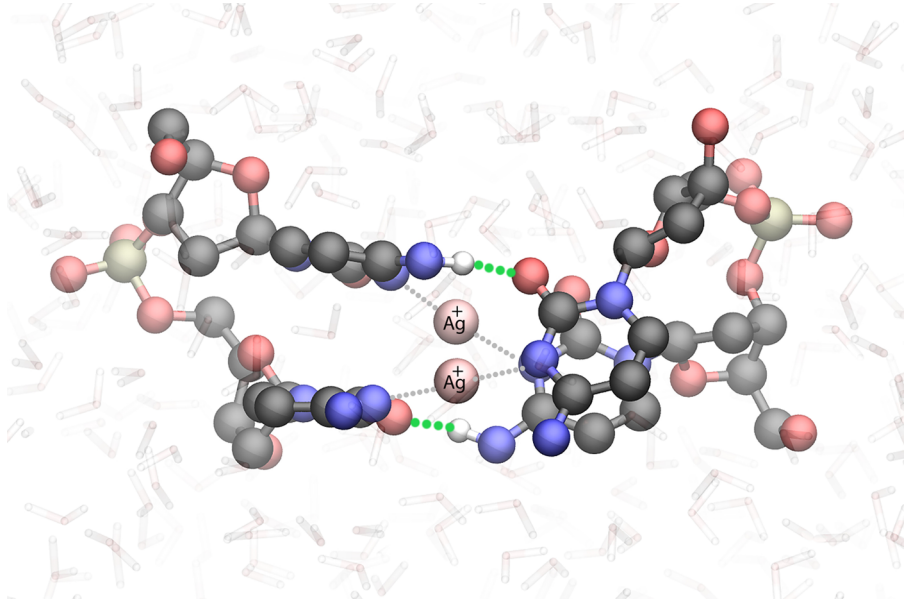

Figure 3. One solvated structure from the final 0.5 ps of the QM/MM run. The quantum region in the simulation includes the full tetramer and 10 water molecules. The interplanar H-bonds are highlighted with a green dashed line and a gray line indicates the Ag–N bonds. Other hydrogen atoms than those involved in the interplanar bond are removed for clarity.

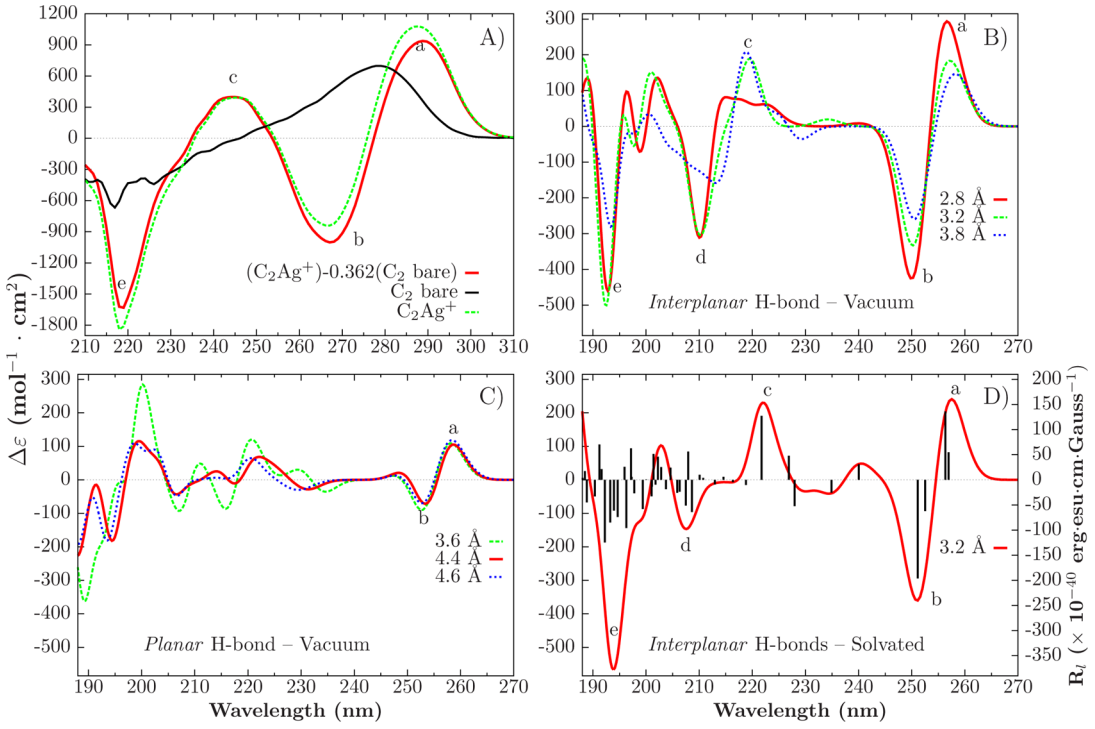

Figure 4. (A) Experimental ECD for the bare C_2 strand solution (black), for the C_2Ag^+ solution (green), and for the estimated contribution of the Ag^+-bridged cytosine tetramer only (red). (B) Vacuum interplanar H-bond ECD spectrum at various Ag–Ag distances. The lowest energy structure is solid red. (C) Vacuum planar H-bond ECD spectrum at various Ag–Ag distances. The lowest energy structure is solid red. (D) Solvated model ECD spectrum (red) with rotatory strengths as sticks (black).

distances, while the planar H-bond stabilizes the tetramer at long Ag–Ag distances.

Experimentally, Ag^+-bridged cytosine tetramer structures are stable in the gas phase as evidenced by mass spectrometry (see SI). Our calculations predict that in such conditions there are two stable configurations for the Ag^+-bridged cytosine tetramer. One configuration has argentophilic interaction, with an interplanar H-bond that could yield completely new types of 3D structures. The other configuration, with planar H-bonds and no argentophilic interaction, has a wide interbase and interplane free space that can potentially be used as a host space for clusters or other molecules. For the more practically important case of aqueous solution, it is important to determine the hydration effect on these structures, as we discuss next.

To test the effects of water, we performed calculations on the Ag^+-bridged tetramer using the QM/MM methodology (see

DOI: 10.1021/acs.jpclett.5b01864
J. Phys. Chem. Lett. 2015, 6, 4061–4066

details in the Computational Methods section and SI). The interplanar H-bond structure was initially solvated and thermalized at 300 K with a classical MD run of 400 ps. The QM/MM simulations were performed then for 22 ps and the last 5 ps were used for analysis. The solvated structure at 5 ps of the trajectory is shown in Figure 3. It was found that the Ag−Ag distance oscillates around an average value of 3.5 Å with 0.21 Å standard deviation. The solvated Ag−Ag distance strongly deviates from the gas-phase minima at 2.8 and 4.2 Å for the interplanar and the planar structures, respectively. The distances between the O−H atoms forming the two potential interplanar H-bonds remained mostly bonded (average of 1.91 and 1.81 Å with standard deviation of 0.17 and 0.14 Å, respectively). Moreover, the residence time of the interplanar H-bonds are 81 and 91% calculated with a cutoff of 2 Å. The dihedral angle C2−N3−N3′-C2′ showed a perpendicular disposition between pairs of dimers (dihedral averages of 90° and 71° with standard deviation of 14° and 9° respectively). The solvated structure is therefore similar to the interplanar structure found in vacuum but more symmetric with two H-bonds and a longer Ag−Ag distance in a region where the argentophilic interaction is very weak. In summary, water affects the overall structure by stabilizing the Ag−Ag distance away from the gas-phase minima and into a symmetric interplanar geometry.

To test the relevance of the different simulated structures, we compare their simulated ECD spectra to experiment (Figure 4A). The experimental ECD of solutions containing silver-mediated cytosine tetramers (green, labeled C_2Ag^+) and that of the C_2 dinucleotide strands alone (black) differ strikingly. To correct for the possible presence of unbound C_2 in the C_2Ag^+ solution, we weighted the ECD spectra for the C_2 strands by the relative contributions of the bare strand and the Ag^+-bridged tetramer found in ESI-MS. The red curve in Figure 4A shows the estimated contribution of the Ag^+-bridged tetramer alone, with positive peaks at 287.5 and 245.2 nm, negative peaks at 266.7 and 218 nm, and no detectable structure at wavelengths beyond ∼300 nm.

We used the time-dependent DFT (TDDFT) in our calculation of the ECD, with a long-range corrected exchange-correlation functional (CAM-B3LYP) on the different systems to test the silver-mediated cytosine tetramers simulated geometries. In all cases, we modified the structures (gas phase or solvated) by replacing the sugar−phosphate backbone with hydrogen atoms and then relaxed the hydrogen atoms. The main results including the experimental data are summarized in Figure 4. We have identified five peaks labeled as a, b, c, d and e. The labeling of the experimental data (Figure 4A) suggests the corresponding peaks.

We first performed calculations on the lowest energy gas-phase structures. In Figure 4B, the interplanar structure has overall better agreement to the experiment than the planar one (see Figure 4C). The interplanar ECD main peaks are at 256.6 nm, 250.0 nm, ∼ 218.0 nm, 210.0 and 192.8 nm, labeled a−e, respectively. The interplanar simulated ECD peaks a, b, c, and e follow a similar pattern to the relative positions and signs of the experimental peaks at 287.5, 266.7, 245.2, and 218 nm. The ECD of all the structures obtained from the study in vacuum were also computed (see SI), and they show that the interplanar structure possesses a more stable ECD spectrum when the structure is stretched. The ECD of the planar structure, conversely, has large variation with Ag−Ag distance.

To study solvation effects, we extracted a structure from the last 0.5 ps of the QM/MM run, including the first water solvation shell of the nucleobases and optimized it at the PBE-vdW corrected level. The optimized structure has a final Ag−Ag distance of 3.2 Å and dihedral angles of 129.7° and 104.7°. The optimized Ag−Ag distance is 0.4 Å longer than the gas-phase minima of the interplanar structure. The presence of the water molecules directly interacting with the nucleobases allows the overall structure to relax to a potential energy minimum away from the vacuum one. We use this structure as a representative of the solvated one since it preserves the characteristic solvated longer Ag−Ag distance. The simulated ECD is shown in Figure 4D. It has the same overall good agreement with the experiment as the gas-phase interplanar structure, but it has improved relative intensities. The main peaks of the solvated ECD are 257.5, 251.1, 222.0, 207.5, and 193.7 nm, which can be then related to the experimental a, b, c, and e peaks. Peak d is not resolved in the experiment, and the inclusion of solvent corrects the overestimated intensity present in the vacuum interplanar H-bond ECD spectrum. In general, the calculated peaks are shifted to higher energies relative to experiment by only 6% to 11% in agreement with similar calculations with the same functional.[21] From the ECD comparison we conclude that the careful choice of accurate and realistic methods gives a satisfactory agreement of the interplanar structure to the experiment.

What we discovered is that H-bonds determine the structure of the solvated silver-mediated cytosine tetramer through novel interplanar bonds. This finding provides the opportunity to devise 3D metal-mediated duplexes using the interplanar H-bond as a building block. Future studies should consider longer strands and homopolymers with other nucleobase compositions.

COMPUTATIONAL AND EXPERIMENTAL METHODS

Computational Methods. To calculate the electronic ground state we used DFT with a real space basis and the projector-augmented wave method.[29] The exchange correlation functional PBE+TS09 was chosen to account for vdW dispersion interactions.[25,26] In the SI we document our tests on their performance describing systems where the cation−π or argentophillic interaction is dominant (SI Section 1). The grid spacing was 0.18 Å and the calculation was spin-unpolarized. Per atom, the electronic configuration of the valence electrons are $H(1s^1)$, $O(2s^22p^4)$, $C(2s^22p^2)$, $N(2s^22p^3)$, $Ag(4p^64d^{10}5s^1)$, including a scalar relativistic correction and a frozen core. Simulations of the ECD spectra are performed on PBE+TS09 geometries with TDDFT using the long-range corrected CAM-B3LYP functional. The Gaussian code[30] is used with a LANL2DZ/ECP basis set for the silver atom and aug-cc-pVDZ for the rest.

The QM/MM calculations were performed using the CPMD package,[31] which combines Car−Parrinello MD, based on DFT, with Amber force-field[32,33] used in classical calculations. The QM/MM interface is modeled by the use of a link-atom pseudopotential that saturates the QM region. Norm conserving Goedecker−Teter−Hutter pseudopotentials[34] were used to describe the nuclei and core electrons of the QM atoms. For Ag^+, a 19 valence electron semicore pseudopotential was used. The electronic orbitals were expanded in plane waves using a reciprocal space kinetic energy cutoff of 90 Ry. The total size of the system was 2/118/

DOI: 10.1021/acs.jpclett.5b01864
J. Phys. Chem. Lett. 2015, 6, 4061−4066

2441 Ag, tetramer and water atoms, respectively. The electrostatic interactions between the QM and MM regions were handled via a fully Hamiltonian coupling scheme,[35] where the short-range electrostatic interactions between the QM and the MM regions are explicitly taken into account for all atoms. An appropriately modified Coulomb potential was used to ensure that no unphysical escape of the electronic density from the QM to the MM region occurs. The electrostatic interactions with the more distant MM atoms were treated via a multipole expansion. Bonded and van der Waals interactions between the QM and the MM regions were treated with the standard AMBER force field. Long-range electrostatic interactions between MM atoms were described with the P3M implementation[36] using a 64 × 64 × 64 mesh. Analysis of the trajectories was carried out using standard tools of the VMD program.[37] QM/MM MD simulations were performed without any restriction on the motion of tetramer, silver ions, and solvent. Further computational details are given in the SI.

Experimental Section. The cytosine dinucleotide, C_2, was ordered from Trilink BioTechnologies at a reported 95%+ purity and used without further purification. Analytical grade $AgNO_3$ and ammonium acetate were purchased from Sigma-Aldrich. All solutions were prepared using Integrated DNA Technologies nuclease free water. All solutions containing DNA were annealed at 90 °C for 5 min and allowed to slowly cool to room temperature prior to analysis. Samples for ESI-MS were prepared in 10 mM ammonium acetate buffer at pH 7.0. The solutions contained 40 μM DNA and $AgNO_3$ at a 1 Ag^+/base ratio. The dinucleotide solutions were injected into the MS (Waters QTOF2) at 10 μL/min in ESI negative mode with a 2 kV capillary voltage, 30 V cone voltage and 14 V collision energy. The signal was integrated over approximately 5 min. The ECD spectra were collected on an Aviv 202 circular dichrometer at 25 °C. Solutions contained 40 μM DNA in a 7.5 mM MOPS buffer at pH 7.0. Ag^+-bridged cytosine tetramers were formed by the addition of $AgNO_3$ at 1 Ag^+/base.

■ ASSOCIATED CONTENT

Supporting Information

The Supporting Information is available free of charge on the ACS Publications website at DOI: 10.1021/acs.jpclett.5b01864.

Computational details on the use of van der Waals DFT correction, Minima Hopping search algorithm, hybrid quantum mechanics classical mechanics simulations, and the calculation of electronic circular dichroism. Experimental details on the mass spectrometry and electronic circular dichroism measurements. (PDF)

■ AUTHOR INFORMATION

Corresponding Author

*E-mail: olga.lopez.acevedo@aalto.fi.

Notes

The authors declare no competing financial interest.

■ ACKNOWLEDGMENTS

The authors thank Mercedes Alfonso-Prieto for aid during the QM/MM simulations. This work was supported by the Academy of Finland Projects 279240 and 251748, by the NSF Grant NSF-CHE-1213895, by MINECO Grant CTQ2014-55174 and by AGAUS Grant 2014SGR-987. We are grateful to CSC, the Finnish IT Center for Science in Espoo, and the Applied Physics Department of Aalto University for computational resources.

■ REFERENCES

(1) Mallajosyula, S.; Pati, S. Conformational Tuning of Magnetic Interactions in Metal-DNA Complexes. *Angew. Chem., Int. Ed.* **2009**, *48*, 4977−4981.

(2) Copp, S. M.; Schultz, D. E.; Swasey, S.; Gwinn, E. G. Atomically Precise Arrays of Fluorescent Silver Clusters: A Modular Approach for Metal Cluster Photonics on DNA Nanostructures. *ACS Nano* **2015**, *9*, 2303−2310.

(3) Copp, S. M.; Bogdanov, P.; Debord, M.; Singh, A.; Gwinn, E. Base Motif Recognition and Design of DNA Templates for Fluorescent Silver Clusters by Machine Learning. *Adv. Mater.* **2014**, *26*, 5839−5845.

(4) Yuen, L. H.; Franzini, R. M.; Wang, S.; Crisalli, P.; Singh, V.; Jiang, W.; Kool, E. T. Pattern-Based Detection of Toxic Metals in Surface Water with DNA Polyfluorophores. *Angew. Chem., Int. Ed.* **2014**, *53*, 5361−5365.

(5) Obliosca, J. M.; Liu, C.; Batson, R. A.; Babin, M. C.; Werner, J. H.; Yeh, H.-C. DNA/RNA Detection Using DNA-Templated Few-Atom Silver Nanoclusters. *Biosensors* **2013**, *3*, 185−200.

(6) Gwinn, E.; Schultz, D.; Copp, S. M.; Swasey, S. DNA-Protected Silver Clusters for Nanophotonics. *Nanomaterials* **2015**, *5*, 180−207.

(7) Yang, H.; Metera, K. L.; Sleiman, H. F. DNA Modified with Metal Complexes: Applications in the Construction of Higher Order Metal-DNA Nanostructures. *Coord. Chem. Rev.* **2010**, *254*, 2403−2415. Supramolecular Approaches to Nano and Molecular Electronics

(8) Xiang, Y.; Lu, Y. DNA as Sensors and Imaging Agents for Metal Ions. *Inorg. Chem.* **2014**, *53*, 1925−1942.

(9) Sinha, I.; Fonseca-Guerra, C.; Müller, J. A Highly Stabilizing Silver(I)-Mediated Base Pair in Parallel-Stranded DNA. *Angew. Chem., Int. Ed.* **2015**, *54*, 3603−3606.

(10) Johannsen, S.; Megger, N.; Böhme, D.; Sigel, R. K.; Müller, J. Solution Structure of a DNA Double Helix with Consecutive Metal-Mediated Base Pairs. *Nat. Chem.* **2010**, *2*, 229−234.

(11) Mandal, S.; Hepp, A.; Müller, J. Unprecedented Dinuclear Silver(I)-Mediated Base Pair Involving the DNA Lesion 1,N^6-Ethenoadenine. *Dalton Trans.* **2015**, *44*, 3540−3543.

(12) Ono, A.; Cao, S.; Togashi, H.; Tashiro, M.; Fujimoto, T.; Machinami, T.; Oda, S.; Miyake, Y.; Okamoto, I.; Tanaka, Y. Specific Interactions Between Silver(I) Ions and Cytosine-Cytosine Pairs in DNA Duplexes. *Chem. Commun.* **2008**, 4825−4827.

(13) Megger, D. A.; Müller, J. Silver(I)-Mediated Cytosine Self-Pairing is Preferred Over Hoogsteen-Type Base Pairs with the Artificial Nucleobase 1,3-Dideaza-6-Nitropurine. *Nucleosides, Nucleotides Nucleic Acids* **2010**, *29*, 27−38.

(14) Swasey, S. M.; Leal, L. E.; Lopez-Acevedo, O.; Pavlovich, J.; Gwinn, E. G. Silver(I) as DNA Glue: Ag^+-Mediated Guanine Pairing Revealed by Removing Watson-Crick Constraints. *Sci. Rep.* **2015**, *5*, 10163.

(15) Megger, D. A.; Fonseca Guerra, C.; Bickelhaupt, F. M.; Müller, J. Silver(I)-mediated Hoogsteen-type base pairs. *J. Inorg. Biochem.* **2011**, *105*, 1398−1404.

(16) Espinosa Leal, L. A.; Lopez-Acevedo, O. On The Interaction Between Gold and Silver Metal Atoms and DNA/RNA Nucleobases-A Comprehensive Computational Study of Ground State Properties. *Nanotechnol. Rev.* **2015**, *4*, 173−191.

(17) Scharf, P.; Müller, J. Nucleic Acids With Metal-Mediated Base Pairs and Their Applications. *ChemPlusChem* **2013**, *78*, 20−34.

(18) Schmidbaur, H.; Schier, A. Argentophilic Interactions. *Angew. Chem., Int. Ed.* **2015**, *54*, 746−784.

(19) Kondo, J.; Yamada, T.; Hirose, C.; Okamoto, I.; Tanaka, Y.; Ono, A. Crystal Structure of Metallo DNA Duplex Containing Consecutive Watson-Crick-like T-Hg(II)-T Base Pairs. *Angew. Chem., Int. Ed.* **2014**, *53*, 2385−2388.

(20) Munksgaard Nielsen, L.; Holm, A. I. S.; Varsano, D.; Kadhane, U.; Hoffmann, S. V.; di Felice, R.; Rubio, A.; Brøndsted Nielsen, S. Fingerprints of Bonding Motifs in DNA Duplexes of Adenine and

DOI: 10.1021/acs.jpclett.5b01864
J. Phys. Chem. Lett. 2015, 6, 4061−4066

Thymine Revealed from Circular Dichroism: Synchrotron Radiation Experiments and TDDFT Calculations. *J. Phys. Chem. B* **2009**, *113*, 9614−9619.
(21) Di Meo, F.; Pedersen, M. N.; Rubio-Magnieto, J.; Surin, M.; Linares, M.; Norman, P. DNA Electronic Circular Dichroism on the Inter-Base Pair Scale: An Experimental-Theoretical Case Study of the AT Homo-Oligonucleotide. *J. Phys. Chem. Lett.* **2015**, *6*, 355−359.
(22) McAlexander, H. R.; Crawford, T. D. Simulation of Circularly Polarized Luminescence Spectra Using Coupled Cluster Theory. *J. Chem. Phys.* **2015**, *142*, 154101.
(23) Klimeš, J.; Michaelides, A. Perspective: Advances and Challenges in Treating van der Waals Dispersion Forces in Density Functional Theory. *J. Chem. Phys.* **2012**, *137*, 120901.
(24) Fortino, M.; Marino, T.; Russo, N. Theoretical Study of Silver-Ion-Mediated Base Pairs: The Case of C-Ag-C and C-Ag-A Systems. *J. Phys. Chem. A* **2015**, *119*, 5153−5157.
(25) Perdew, J. P.; Burke, K.; Ernzerhof, M. Generalized Gradient Approximation Made Simple. *Phys. Rev. Lett.* **1996**, *77*, 3865−3868.
(26) Tkatchenko, A.; Scheffler, M. Accurate Molecular Van Der Waals Interactions from Ground-State Electron Density and Free-Atom Reference Data. *Phys. Rev. Lett.* **2009**, *102*, 073005.
(27) Otero-de-la Roza, A.; Mallory, J. D.; Johnson, E. R. Metallophilic interactions from dispersion-corrected density-functional theory. *J. Chem. Phys.* **2014**, *140*, 18A504.
(28) Goedecker, S. Minima Hopping: An Efficient Search Method for the Global Minimum of the Potential Energy Surface of Complex Molecular Systems. *J. Chem. Phys.* **2004**, *120*, 9911.
(29) Enkovaara, J.; Rostgaard, C.; Mortensen, J. J.; Chen, J.; Dułak, M.; Ferrighi, L.; Gavnholt, J.; Glinsvad, C.; Haikola, V.; Hansen, H. A.; et al. Electronic Structure Calculations with GPAW: A Real-Space Implementation of the Projector Augmented-Wave Method. *J. Phys.: Condens. Matter* **2010**, *22*, 253202.
(30) Frisch, M. J.; Trucks, G. W.; Schlegel, H. B.; Scuseria, G. E.; Robb, M. A.; Cheeseman, J. R.; Scalmani, G.; Barone, V.; Mennucci, B.; Petersson, G. A. et al. *Gaussian 09*, revision D.0;. Gaussian, Inc.: Wallingford, CT, 2009.
(31) CPMD; http://www.cpmd.org/. Copyright IBM Corp 1990−2015, Copyright MPI für Festkörperforschung Stuttgart 1997−2001.
(32) Cornell, W. D.; Cieplak, P.; Bayly, C. I.; Gould, I. R.; Merz, K. M.; Ferguson, D. M.; Spellmeyer, D. C.; Fox, T.; Caldwell, J. W.; Kollman, P. A. A Second Generation Force Field for the Simulation of Proteins, Nucleic Acids, and Organic Molecules. *J. Am. Chem. Soc.* **1995**, *117*, 5179−5197.
(33) Pérez, A.; Marchán, I.; Svozil, D.; Sponer, J.; Cheatham, T. E.; Laughton, C. A.; Orozco, M. Refinement of the AMBER Force Field for Nucleic Acids: Improving the Description of α/γConformers. *Biophys. J.* **2007**, *92*, 3817−3829.
(34) Goedecker, S.; Teter, M.; Hutter, J. Separable dual-space Gaussian pseudopotentials. *Phys. Rev. B: Condens. Matter Mater. Phys.* **1996**, *54*, 1703−1710.
(35) Laio, A.; VandeVondele, J.; Rothlisberger, U. A Hamiltonian Electrostatic Coupling Scheme for Hybrid Car-Parrinello Molecular Dynamics Simulations. *J. Chem. Phys.* **2002**, *116*, 6941−6947.
(36) Jorgensen, W.; Chandrasekhar, J.; Madura, J.; Impey, R.; Klein, M. Comparison of Simple Potential Functions for Simulating Liquid Water. *J. Chem. Phys.* **1983**, *79*, 926−935.
(37) Humphrey, W.; Dalke, A.; Schulten, K. VMD - Visual Molecular Dynamics. *J. Mol. Graphics* **1996**, *14*, 33−38.

DOI: 10.1021/acs.jpclett.5b01864
J. Phys. Chem. Lett. 2015, 6, 4061−4066